

Size Effect Aspects of Measurement of Fracture Characteristics of Quasibrittle Material

Zdeněk P. Bažant

Northwestern University, Evanston, Illinois

This paper, which represents the text of an introductory report presented at Cardiff workshop in 1995, reviews the size effect from two different viewpoints: (1) the need to eliminate or minimize the effect of specimen size on the measured material fracture characteristics, and (2) the exploitation of measured size effect on the nominal strength for determining the material fracture characteristics. Three methods of fracture testing are examined in the perspective of the size effect, and the merits and weaknesses of various methods in regard to the size effect are pointed out. The parameters of all three methods can be determined by simple formulas and linear regression from measurements allowing calibration of two parameters of the size effect law. ADVANCED CEMENT BASED MATERIALS 1996, 4, 128–137

KEY WORDS: Concrete, Fracture mechanics, Fracture testing, Scaling, Size effect, Standardization, Test specimens, Quasibrittle materials

The size effect on nominal strength of structures is the most important practical consequence of the global energy release associated with large fractures. Therefore, it is natural to exploit the size effect for measuring the material fracture properties. At the same time, the measured values of the parameters characterizing material properties must be independent of the specimen or structure size, or they would not represent only the properties of the material but also the properties of the structure.

The objective of the present paper, which represents the text of an introductory report that was orally presented at the size effect session of a recent workshop in

Cardiff¹ on the subject and was summarized at a subsequent workshop at FraM CoS-2,² is to review the issues that were deemed³ to be most important or interesting for the problem of selecting a standardized fracture test. Presentation of a comprehensive state-of-the-art report, mathematical derivations, and experimental validations are not the objective. No claims for exhaustiveness of the present review are made. Design and other aspects of size effect are not covered in this paper.

Two Aspects of Size Effect

The size effect impacts the problem of choice of a standardized fracture test in two ways:

1. *Size Independence of Fracture Characteristics: Objectivity Requirement*—The material fracture parameters such as the fracture energy must be independent of the specimen size (and geometry) when geometrically similar specimens of different sizes are tested. It is the basic requirement of objectivity of a fracture model.
2. *Determination of Fracture Parameters from Size Effect Measurements*—Measurement of the size effect on nominal strength of concrete specimens can be ex-

¹NSF Workshop on Standards for Measurement of Mode I Fracture Properties of Concrete, organized by B.I.G. Barr and S. Swartz, University of Wales, Cardiff, July 20–21, 1995.

²Workshop, coordinated by P. Rossi, on "Size Effects: Theoretical Concepts, Experimental Verification, and Implications for Design" at 2nd International Conference on Fracture Mechanics of Concrete and Concrete Structures (FraMCoS-2), chaired by F.H. Wittmann, E.T.H., Zürich, July 26, 1995.

³Based on the reporter's correspondence before Cardiff workshop with the members of Working Group 3, having Z.P. Bažant and B. Karihaloo as co-chairmen and W. Gerstle, A. Maji, H. Mihashi, P. Perdikaris, V. Saouma, T. Tang, and M. Tasdemir as members.

Address correspondence to: Dr. Zdeněk P. Bažant, W.P. Murphy Professor of Civil Engineering and Materials Science, Northwestern University, Room Tech A131, Evanston, Illinois 60208.

Received August 14, 1995; Accepted January 9, 1996

ploited for determining the fracture parameters. It is in fact desirable to do so because the size effect is the most important feature of fracture mechanics of quasibrittle materials, distinguishing it from other failure theories, and it is the main reason why fracture mechanics needs to be introduced into design. If designers are concerned mainly about size effect, they should calibrate the material parameters on the basis of the measured size effect.

Test Methods and Their Parameters

Work-of-Fracture Method

The work-of-fracture method (ACI 1992) [1], proposed for ceramics by Nakayama [2] and Tattersall and Tappin [3], was developed for concrete by Hillerborg [4]. It is based on the cohesive (or fictitious) crack model proposed for concrete by Hillerborg et al. [5]. This model is characterized by a stress-displacement curve $\sigma = \varphi(\omega)$ relating the cohesive (crack-bridging) stress σ to the crack-opening displacement ω . The two main parameters of the curve $\varphi(\omega)$ are: (1) the area under the complete curve, representing the fracture energy G_f^H (superscript *H* referring to Hillerborg), and (2) the initial slope of the curve that may be characterized by the area under the initial tangent representing the initial fracture energy G_f^I (Figure 1). According to Planas, Elices, and Guinea [6], one can also approximately identify as the third parameter the center of gravity of the area under the $\phi(v)$ curve, and the three parameters then suffice to uniquely characterize a bilinear softening curve $\phi(v)$. The more detailed characteristics of the curve $\varphi(\omega)$ have little effect on the predicted fracture behavior of structures and can hardly be experimentally determined without ambiguity. So (aside from parameters E and f_t , which do not refer exclusively to fracture), the number of fracture parameters that can be meaningfully determined by this method is basically two, although perhaps a third parameter can be identified from tests in a crude approximate manner.

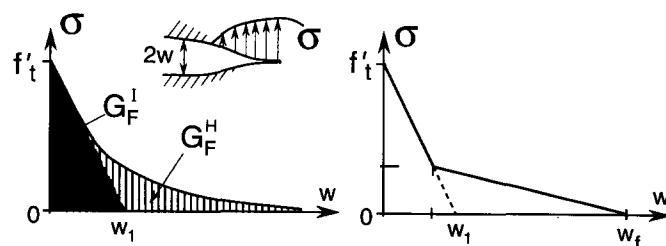


FIGURE 1. Softening stress-displacement law of cohesive (fictitious) crack model and its bilinear idealization.

Size Effect Method

In the size effect method [7], proposed for measuring fracture energy by Bažant [8,9] and for measuring two fracture parameters by Bažant and Kazemi [10], the basic fracture characteristics are: (1) the fracture energy, G_f^s (with superscript *s* referring to size effect method), and (2) the effective length of fracture process zone, c_f , defined as the distance from the notch tip to the tip of the equivalent linear elastic fracture mechanics (LEFM) crack in a specimen mathematically extrapolated to infinite size. The method is based on the size effect law proposed by Bažant [11,12] and particularly on its special form in terms of G_f^s and c_f and the dimensionless energy release rate function $g(\alpha)$, accounting for geometry, as proposed by Bažant and Kazemi [10,13].

Jenq-Shah Method

This method is based on a fracture model proposed for concrete by Jenq and Shah [14], which is mathematically similar to the Wells-Cottrell [15,16] model for metals but has a very different underlying physical mechanism, with no plasticity. Same as the foregoing two models, this model contains two material fracture parameters: (1) the fracture toughness, K_{Ic}^{JS} (with superscript *JS* referring to Jenq and Shah), and (2) the critical crack-tip opening displacement δ_{CTOD}^S , which represents the opening displacement at the tip of notch (provided the fracture process zone remains attached to the notch). Instead of K_{Ic}^{JS} , one can use the fracture energy $G_f^{JS} = (K_{Ic}^{JS})^2/E'$ as one of the basic parameters.

Each of the fracture models underlying these methods is nonlinear and is completely or essentially defined by two parameters (G_f and f_t , or G_f and c_f or G_f and δ_{CTOD}^S). By contrast, LEFM has only one material parameter, either G_f or $K_{Ic} = \sqrt{E'G_f}$.

Extrapolation to Infinite Size

Every test method is inevitably based on some material fracture model. A practical fracture model of quasibrittle material represents a simplified description of a very complex process of progressive material damage and its localization in the fracture process zone. For this reason, the parameters of any available fracture model serving as a basis of standardized test can be truly unambiguously defined only by extrapolation to infinite size. Indeed, in a specimen of infinite size, the fracture process zone is negligibly small compared to the specimen size, which implies LEFM to be applicable. This in turn implies that the displacement field to which the fracture process zone is exposed along its boundary is the near-tip LEFM displacement field. This field is the same for any specimen geometry. Because the stress

and strain fields in the interior of the fracture process zone must depend (in the sense of continuum smoothing) on the boundary displacements uniquely, they must also be the same. This guarantees the material fracture parameters defined on the basis of extrapolation to infinite size to be shape independent and, of course, size independent.

Thus, strictly speaking, an unambiguous definition of G_f^s , G_f^H , G_f^I , G_f^{IS} , c_f , K_{Ic} , and δ_{CTOD} as true material properties, independent of specimen geometry and size, can be given only on the basis of extrapolation to infinite size.

Requirement of Size Independence of Fracture Model Parameters

The fracture parameters obtained from the size effect law are, by definition, size independent. This is true not only for the specimens of the geometry used in tests but also for specimens of other geometries, because the same size effect law was shown to apply to specimens of very different geometries.

The parameters of the Jenq and Shah model determined from the size effect law are of course size independent. If they are determined in the originally proposed way (with direct crack-tip opening displacement measurements), they appear to be approximately independent of the specimen size.

The fracture energy G_f^H , measured according to the work-of-fracture method on the basis of the area under the complete load-deflection curve of the specimen, was shown to be significantly size dependent. This appears to be a weakness of the cohesive crack model. The sources of this size dependence have been carefully analyzed by Guinea, Planas, and Elices [19,20], who also suggested how the size dependence of G_f^H could be mitigated.

As for G_f^I , it may be expected to be essentially size independent because it is approximately equal to G_f^s , which is size independent. Thus, the size dependence of G_f^H appears to be caused by the tail of the stress-displacement curve. The size dependence implies that the stress-displacement curve $\varphi(\omega)$ cannot be unique, contrary to the basic hypothesis of the cohesive crack model.

Ease of Determination of R-Curve for Given Structure Geometry

Other fracture characteristics, such as the R-curve, can be obtained from the aforementioned fracture characteristics. The R-curve, allowing the use of LEFM, represents the basis of the simplest method of structural

analysis for fracture. Thus, it is desirable that the fracture model would yield the R-curve in the most direct way possible.

This is achieved by the size effect method, for which the R-curve can be obtained from simple explicit expressions on the basis of G_f , c_f and the known energy release function for the given structure geometry. The formulas ensue from the size effect law because the R-curve is simply the envelope of fracture equilibrium curves for specimens of different sizes.

When the Jenq-Shah model is used, the value of δ_{CTOD} may first be converted to c_f and then the R-curve can be calculated from the size effect by a known procedure. Another way, which is however equivalent, omits the explicit calculation of c_f and uses formulas giving the R-curve directly [17].

For the cohesive crack model, determination of the R-curve (curve of critical energy release rate R versus LEFM equivalent crack length a) is difficult; it requires nonlinear finite element analysis, which seems to be a disadvantage of this fracture model. Nevertheless, a different type of R-curve, namely R versus CTOD, can be approximately calculated in a closed form [19,20,21].

Size Effect Method of Testing Material Fracture Parameters

The main advantage of the size effect method of measuring material fracture characteristics is the simplicity of measurement. Only the maximum loads of specimens need to be measured. For this purpose, sophisticated closed-loop systems and a stiff testing frame are not necessary. The measurements can be carried out in any laboratory, with the simplest equipment, and can be carried out even in the field, as demonstrated at the Texas Transportation Institute [22].

The second advantage of the size effect method is that the measurements are based on the same effect as that needed most for structural design. The model is calibrated by the effect that it is intended to predict.

In the original form proposed in 1987 [8,9], the size effect method has been amply verified and is now supported by broad experimental evidence. Recently, in an effort to make testing more convenient, three new versions of the size effect method have been formulated, and so four versions exist at present.

Original Version With Geometrically Similar Specimens of Different Sizes (Type I)

In the originally proposed version [8,9], adopted as one of the RILEM recommendations [23], geometrically similar specimens of different sizes, spanning the size ratio of at least 1:4, are tested. G_f^s and c_f are then deter-

mined either by nonlinear optimization or linear regression, along with their coefficients of variation.

For the original version, the size effect method has a third advantage: The identification of material parameters can be reduced to linear regression, and the regression can be arranged in such a way that the slope of the regression line gives the fracture energy. Linear regression is the most effective way to obtain good statistics, such as the coefficient of variation of the fracture energy, and the statistics are most dependable when the quantity of interest is the regression slope, as is the case for G_f^s .

For a material exhibiting such a high random scatter as concrete, determining the coefficients of variation of G_f and c_f is important. The design of structures should properly take this statistical information into account. It is one advantage of the size effect method that it makes determination of these coefficients of variation reliable and easy.

One-Size Version Using Zero-Size Strength (Type II)

In this recently proposed version, the maximum loads (or nominal strengths σ_N) of fracture specimens of only one size (and one geometry) are measured, and the nominal strength σ_p at zero-size (plastic) limit for specimens of this geometry is calculated according to plasticity from a known value of tensile strength f_t . Then, using the size effect law, one finds that the fracture characteristics can be calculated from the formulas:

$$G_f = \frac{\sigma_p^2 D_0}{c_n^2 E} g(\alpha_0), \quad c_f = \frac{g(\alpha_0)}{g'(\alpha_0)} D_0 \quad (1)$$

$$D_0 = \frac{D}{(\sigma_p/\sigma_N)^2 - 1} \quad (2)$$

and the nominal strength is defined as $\sigma_N = c_n P_{max}/bD$ where c_n is a factor chosen for convenience. The value of σ_p can be easily calculated according to Mohr-Coulomb yield criterion, assuming a bi-rectangular stress distribution along the ligament of the specimen, with stresses on one and the other end equal to the tensile and compressive strengths. An ongoing research at Northwestern University by Zhengzhi Li [24] has already shown that, for tensile strength equal to f_r , this method works very well for notched three-point-bend concrete fracture specimens of span-to-depth ratio 2.5 and gives results in good agreement with the original size effect method proposed by Bažant and Pfeiffer [8,9], provided that the notched specimens are large enough (a depth of 6 inches appears to suffice, but the larger the better).

There is, however, one aspect that must be handled empirically. The value of tensile yield strength f_t' , which

is needed for calculating σ_p according to plasticity, is not predicted by fracture mechanics. By virtue of approaching for small sizes a horizontal asymptote, the size effect law implies σ_p to correspond to strength theory or plasticity but does not imply the proper value of f_t' to be the direct tensile strength nor to be the same for various specimen geometries. In fact, upon equating the zero size limit $\sigma_p = B_p f_t'$ to $c_n [EG_f/c_f g'(\alpha_0)]^{1/2}$ where $B_p = B_p(\alpha_0)$ = nominal structure strength for unit value of material tensile yield strength calculated according to plasticity, one must conclude that the tensile yield strength value to be used must satisfy the relation:

$$f_t' = c_n \sqrt{EG_f/c_f g'(\alpha_0)}/B_p(\alpha_0) \quad (3)$$

This value is not constant. It varies with specimen geometry. Therefore, it is by chance that good results for the aforementioned specimens are obtained with $f_t' = f_r$ = modulus of rupture. For different geometries, different values of f_t' have to be used (e.g., $1.3 f_r$ or $0.8 f_r$). They would have to be calibrated empirically for the geometry to be specified for the standard testing method. Although this is not difficult to do, it does mean that this method does not have a complete theoretical foundation but contains an empirical ingredient. This feature is not surprising because the size effect law $\sigma_N \propto [1 + (D/D_0)]^{-1/2}$ is valid only within the approximate range $0.22 \leq D/D_0 \leq 4.5$, which excludes zero size.

One-Size Version Using Notchless Specimen Strength (Type III)

The aforementioned empirical ingredient can be avoided at the cost of slightly more complicated calculations. Instead of the zero size limit, one can experimentally determine the strength of a notchless specimen, preferably (but not necessarily) of the same size and shape. This is similar to the standardized test of modulus of rupture, f_r . The size effect on f_r (Appendix 2) [25,26] must of course be taken into account simultaneously with the size effect for notched specimens. This can be accomplished by fitting the maximum load data with the universal size effect law in eq 12 of Appendix 1, which is valid for both notched and notchless specimens. Under the assumption that $D_0 \gg D_b$ where D_b = thickness of the boundary layer in the modulus of rupture test (roughly one maximum aggregate size), which is normally satisfied, the universal law has recently been derived as the matched asymptotic satisfying the following asymptotic properties:

1. For notched specimens and $D \gg D_0$, it agrees with the first three terms of the large size asymptotic series expansion and approaches the LEFM asymptote of slope $-1/2$ as $D \rightarrow \infty$.

2. For notched specimens and $D \ll D_0$, it agrees with the first two terms of the small-size asymptotic expansion and approaches a horizontal asymptote as $D \rightarrow 0$.
3. For notchless specimens, it reduces to the recently derived size effect for the modulus of rupture, agreeing well with test data [26].

Because this law differs from the original size effect law, the optimum fit of the classical data for notched specimens of different sizes [9] is not exactly the same as published, but it is very close.

The fitting of eq 12 to the measured nominal strength of notched and notchless specimens cannot be accomplished by linear regression. However, a computer library subroutine, such as Levenberg-Marquardt nonlinear optimization algorithm, readily yields the values of G_f and c_f that provide the best fit.

Alternatively, iteration of linear regressions can also be used. Equation 12 can be rearranged to the linear form $Y = AX + C$ in which

$$X = \frac{g}{g'} D, \quad Y = \frac{Ec_n^2}{g' \sigma_N^2} \chi, \tag{4}$$

$$\chi = \left\{ 1 + \left[\left(\eta + \frac{4g'D}{-g''c_f} \right) \left(1 + \frac{gD}{g'c_f} \right) \right]^{-1} \right\}^2$$

and $A = 1/G_f$, $C = c_f/G_f$ (note that for $\alpha_0 = 0$ we have $g = 0$ and $X = 0$). Parameter χ is assumed 1 for the first iteration and its value is then updated after each iteration of the linear regression. At Northwestern University, Zhengzhi Li [24] has already established that the iterations converge very well and that this method, which has a consistent theoretical foundation, gives excellent results, very close to those obtained by Bažant and Pfeiffer [9] with the original size effect method. Again, the higher the brittleness number of the notched specimens, the better the results. The specimen geometry and notch length should be chosen to minimize D_0 , that is, the ratio g'/g .

One-Size Version Using Notches of Different Length (Type IV)

As a generalization of the original size effect method, the specimens need not be geometrically similar if the generalized size effect law in terms of $g(\alpha)$, G_f , and c_f [10] is used. However, the range of brittleness numbers $\beta = D/D_0$ must again be at least 1:4.

This formula offers the possibility of identifying material fracture parameters from the maximum loads of specimens of only one size and the same external shape. This has recently been studied in depth by Tang et al. [22] with nearly full success. However, it is not easy to

achieve in this manner a sufficient range of β . Tang succeeded with eccentric compression specimens to achieve a range of about 1:4, which is the minimum required for meaningful approximate results. However, a notch as short as one-eighth of the cross-section depth had to be included to achieve this range of β . From recent research leading to eq 12, it appears that, for such a short notch, the simple size effect law has a significant error, which is according to eq 12 about 14% (approximately the same error magnitude for such a short notch would have to be expected for Jenq-Shah's model because it is approximately equivalent to the size effect law).

It would of course be possible to apply to such short notches the universal size effect law [12], which can describe the transition between specimens with large notches and no notches. But then one may as well use the measurement of the nominal strength of notchless beams, which is the method Type III, and in this way increase at the same time the range of β .

When two sizes of eccentric compression specimens that are similar but have two rather different relative notch depths a_0 are used and the size ratio is 1:2, one can reach a brittleness number range of about 1:6, and for three-point-bend specimens about 1:4 (without using excessively short notches for which the transition to size effect on modulus of rupture would have to be considered). Both ranges are sufficient for measuring G_f and c_f .

Relationship Among Parameters of Different Models

Recently it has been shown that the Jenq-Shah method and the size effect method are mathematically equivalent within the first two terms of the asymptotic series expansion of the dimensionless energy release rate function $g(\alpha)$ in the size effect law. Because the higher order terms of this expansion can get significantly manifested only for size ranges exceeding about 1:20, these two methods must be equivalent for practical purposes and their parameters must be related. Indeed, such a relation has been established [27,28] and may be written as follows:

$$K_{Ic}^S = \sqrt{g(\alpha_0)D_0} Bf'_t = \sqrt{E'G_f^S} \tag{5}$$

$$\delta_{CTOD}^S = \frac{\sqrt{8}}{\pi E'} \sqrt{g(\alpha_0)} g'(\alpha_0) D_0 Bf'_t \tag{6}$$

$$= \frac{\sqrt{8}}{\pi} \frac{K_{Ic}}{E'} \sqrt{c_f} = \frac{\sqrt{8}}{\pi} \sqrt{\frac{G_f^S c_f}{E'}} \tag{6}$$

where Bf'_t and D_0 are parameters of the size effect law $\sigma_N = B f'_t [1 + (D/D_0)]^{-1/2}$, with $\sigma_N = P/bD$ ($c_N = 1$); $E' =$

$E/(1 - \nu^2)$ for plane strain; α_0 = initial relative notch depth; and the values of c_f and G_f^s are the values obtained by fitting maximum load data for notched specimens with the size effect law written in the form:

$$\sigma_N = \sqrt{\frac{E' G_f^s}{g'(\alpha_0)c_f + g(\alpha_0)D}} \quad (7)$$

where D = characteristic dimension (size) of specimen. The calculations are the simplest when the specimens are geometrically similar. However, the specimens need not be geometrically similar, because differences in geometry are captured by different values of $g(\alpha_0)$. Because of the typical scatter of test results for concrete, the range of brittleness numbers $\beta = D/D_0$ must be at least 1:4.

Extensive comparisons of test results by Karihaloo and Nallathambi [29,30] confirmed that

$$G_f^{LS} \approx G_f^s \quad (8)$$

As for the cohesive (fictitious) crack model of Hillerborg et al., it appears that, for normal concrete,

$$G_f^I \approx G_f^s \quad (9)$$

$$G_f^H \approx 2G_f^s \quad (10)$$

which resulted from the simplified theoretical analysis of Planas and Elices [18]. In theory, one should expect G_f^H to be related not only to G_f^s but also to c_f , but this has not yet been researched. In a general cohesive crack model, the ratio G_f^H/G_f^I could of course have any value.

Accurate numerical calculations with the cohesive crack model show that the results closely follow the simple originally proposed size effect law [11,12] within size range 1:20. Thus, the values G_f^s and c_f , which give about the same maximum loads as the cohesive crack model, can be easily obtained by fitting this size effect law to the numerical results with the cohesive crack model. The inverse problem, namely determination of the cohesive crack model from the known size effect law, is more difficult. Nevertheless, it transpires that, approximately, the value of G_f resulting from the size effect law determines the initial slope of the stress-displacement curve, and the value of c_f together with G_f^s ought to decide the area under the complete stress-displacement curve.

To predict the approximate softening stress-displacement curve of Hillerborg's fictitious crack model from size effect data, the curve may be assumed to be bilinear, with a knee at the height about $f_t'/3$ (Figure 1). The initial tangent aims at the point $w = w_1$ on the axis of displacement w , and the second straight line

terminates on the w axis at point w_f . Equations 9 and 10 are satisfied if

$$w_1 = 2G_f^I/f_t', \quad w_f = 2.5w_1 \quad (11)$$

In principle, however, c_f ought to be involved in these relations, but at present it is not known how.

It must be pointed out that for normal laboratory specimens the maximum load values calculated numerically (by finite elements) with the cohesive crack model are insensitive to the tail of the stress-displacement curve defining the cohesive crack model (this might not be quite true for specimens of high strength concrete and strong mortar). These maximum load values are sensitive only to the initial slope of the curve, which means they essentially depend only on G_f^I and not on G_f^H . On the other hand, the size effect on the ductility limit (snapback point on the calculated load-displacement diagram) does depend on G_f^H , but this relationship has not yet been explored systematically.

For a size range 1:1000, accurate finite element calculations of the maximum loads with the cohesive crack model show that a close fit by the size effect law requires its generalized form $\sigma_N = Bf_t'[1 + (D/D_0)^r]^{-1/2r}$ [1,31,32]. For short notch three-point-bend beams, the optimum value is $r \approx 0.45$, but r depends strongly on geometry; for example, for a large panel with a small central crack loaded by pressure on the crack, the optimum value of r appears to be about 1.5. Values of r differing from 1 do not seem important and necessary for the normal size range up to about 1:20.

Conclusion

Knowledge of the size effect on the failure load of fracture specimens, coupled with the effect of shape, is very useful for measuring fracture properties. On the other hand, the effect of size on the values of material fracture parameters must be avoided.

Appendix 1. Universal Size Effect Law and Verification of One-Size Method

The universal size effect law [33,34] applicable to failures at both large cracks and crack initiation from the surface reads:

$$\sigma_N = Bf_r^\infty \left(1 + \frac{D}{D_0}\right)^{-1/2} \left\{1 + \left[\left(\eta + \frac{D}{D_b}\right)\left(1 + \frac{D}{D_0}\right)\right]^{-1}\right\} \quad (12)$$

in which η = empirical constant of the order of 1 and, if we denote $g = g(\alpha_0)$, $g' = g'(\alpha_0)$, $g'_0 = g'(0)$, and $g'' = g''(\alpha_0)$,

$$f_r^c = c_N \sqrt{\frac{EG_f}{c_f g_0'}}, D_0 = \frac{g'}{g} c_f D_b = \frac{\langle -g'' \rangle}{4g'} c_f, B = \sqrt{\frac{g'}{g}} \quad (13)$$

Equation 12 can be proven by expressing σ_N^{-2} in terms of ϑ and expanding it into Taylor series in ϑ about point $\vartheta = 0$. This yields the original size effect law if $\alpha_0 > 0$, and $\sigma_N/f_r^c = 1 + D_b/(D + \eta D_b)$ if $\alpha_0 = 0$. The latter differs from the recently published [35] size effect formula for the modulus of rupture by constant η , but agreement with the first two terms of the asymptotic expansion in D^{-1} is not affected and good fit of test data is not compromised. Introducing constant η achieves that σ_N be finite for $D \rightarrow 0$, for both $\alpha_0 > 0$ and $\alpha_0 = 0$.

Equation 12 represents the matched asymptotic satisfying (1) the first three terms of the large-size expansion in D^{-1} for notched specimens, (2) the first two terms of the small-size expansion in D for the notched specimens, and (3) the first two terms of the large-size expansion in D^{-1} for notchless specimens.

Figure 2 shows the surface of the universal size effect law for a typical three-point-bend specimen (span-to-height ratio = 4). The empty points (circles) in the size effect regression plots in Figures 3 and 4 show the data points from various published size effect tests based on the original size effect method (Type I) and the regression lines of these empty points. The solid (black) points are the mean experimental results for extrapolation to zero size (Type II method, Figure 3) and for notchless specimens (Type III method, Figure 4). The fact that the solid points are rather close to the regression lines of the empty points validates the one-size method. The one-size method graphically means passing a regression

line (not shown) through the solid point and the group of the empty points for one size D only. Obviously, if this is the largest size for each of these test series, this regression line would be almost the same as the regression line of the empty points, and thus nearly the same G_f and c_f values will be obtained as with the original multisize effect method.

Appendix 2. Other Kinds of Size Effect

Weibull Statistical Size Effect

Until about a decade ago, the size effect observed in concrete structures has been universally explained by randomness of strength and calculated according to Weibull theory. Recently, however, it has been shown [35] that this theory cannot apply when large stable fractures can grow in a stable manner prior to maximum load. The main reason is the redistribution of stresses caused by stable fracture growth prior to maximum load and localization of damage into a fracture process zone. If the Weibull probability integral is applied to the redistributed stress field, the dominant contribution comes from the fracture process zone whose size is nearly independent of structure size D . The contribution from the rest of the structure is nearly vanishing, which means the fracture cannot occur outside the process zone. Because this zone has about the same size for specimens of very different sizes, the Weibull-type size effect must, therefore, disappear for large sizes.

A generalized version of Weibull-type theory, in which the material failure probability depends not on the local stress but on the average strain of a characteristic volume of the material, has been shown to yield realistic size effect and also to approach the original size effect law as its deterministic limit [35].

For concrete, Weibull-type size effect might be taking place only in very large structures that fail right at crack initiation, for example, in very deep notchless plain concrete beams. Because for beam depths such as $D = 10D_b$ the stress redistribution in the boundary layer, underlying eq 12, is still significant, the beam depth beyond which the Weibull-type size effect could begin to dominate must be at least $D = 100D_b$. Hardly any case satisfying this condition exists in concrete practice. Besides, good practice requires designing structures so as not to fail at crack initiation. As for notched specimens, the Weibull size effect should, in theory, be approached for very small sizes, but the sizes for which this occurs appear to be too small compared to the aggregate size.

The Question of Possible Role of Fractal Nature of Crack Surface or Microcrack Array

Although the surface roughness of cracks in concrete can be described, within a certain range, by means of a

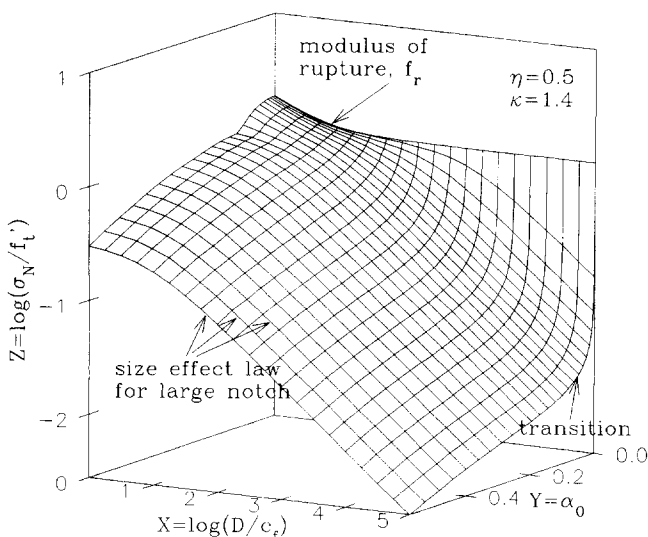


FIGURE 2. Surface of the universal size effect law for notched and notchless specimens.

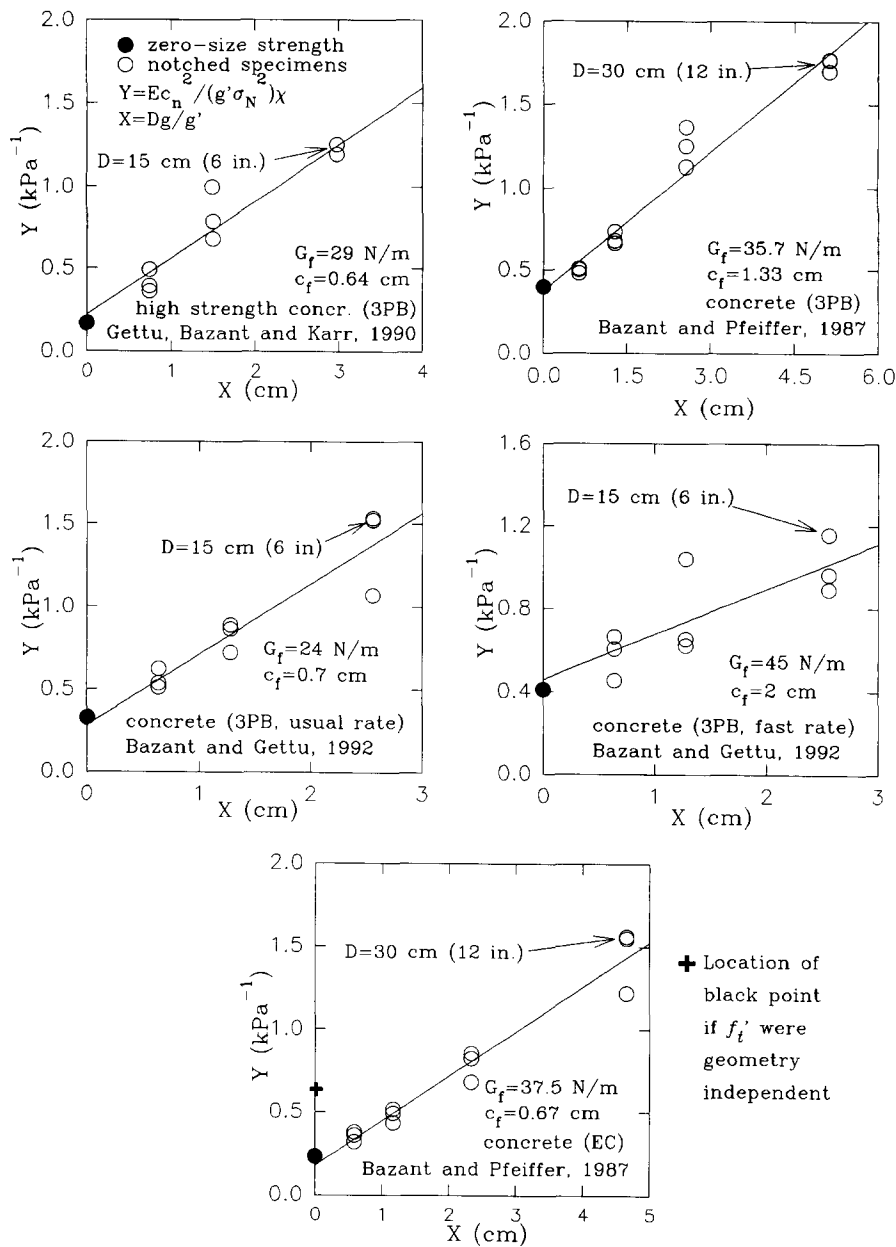


FIGURE 3. Size effect linear regression plots of typical published test data (empty points), their regression lines, and predictions by Type II method for zero size extrapolation.

fractal curve, it appears according to Bažant that the fractality cannot play any significant role in the law of crack propagation and especially not in the observed size effect on σ_N . Two reasons have been offered for this viewpoint [33,34]:

1. The size effect curve derived from the first and second law of thermodynamics disagrees with test data.
2. Distributed microcracking and plastic-frictional slips dissipate a major part of energy at the fracture while the microcracks that eventually become the final macrocrack surface exhibiting fractal features dissipate only a negligible portion of energy.

Since fractal curves such as von Koch's have been cited as paradigms of fractal cracks [36,37], it should further be noted that such curves generally exhibit recessive and spiraling segments that prevent kinematic separation of surfaces. However, this objection can be removed by considering self-affine fractal curves.

To circumvent the aforementioned criticism, it has been suggested [37] that the size effect may be caused by a different type of fractality, namely a lacunar (rarefying) fractal character of the distribution of microcracks in the fracture process zone (for which the fractal dimension is less than the Euclidean dimension). However, it can be shown that this type of fractal hypothesis can lead to nothing else than the Weibull-type size ef-

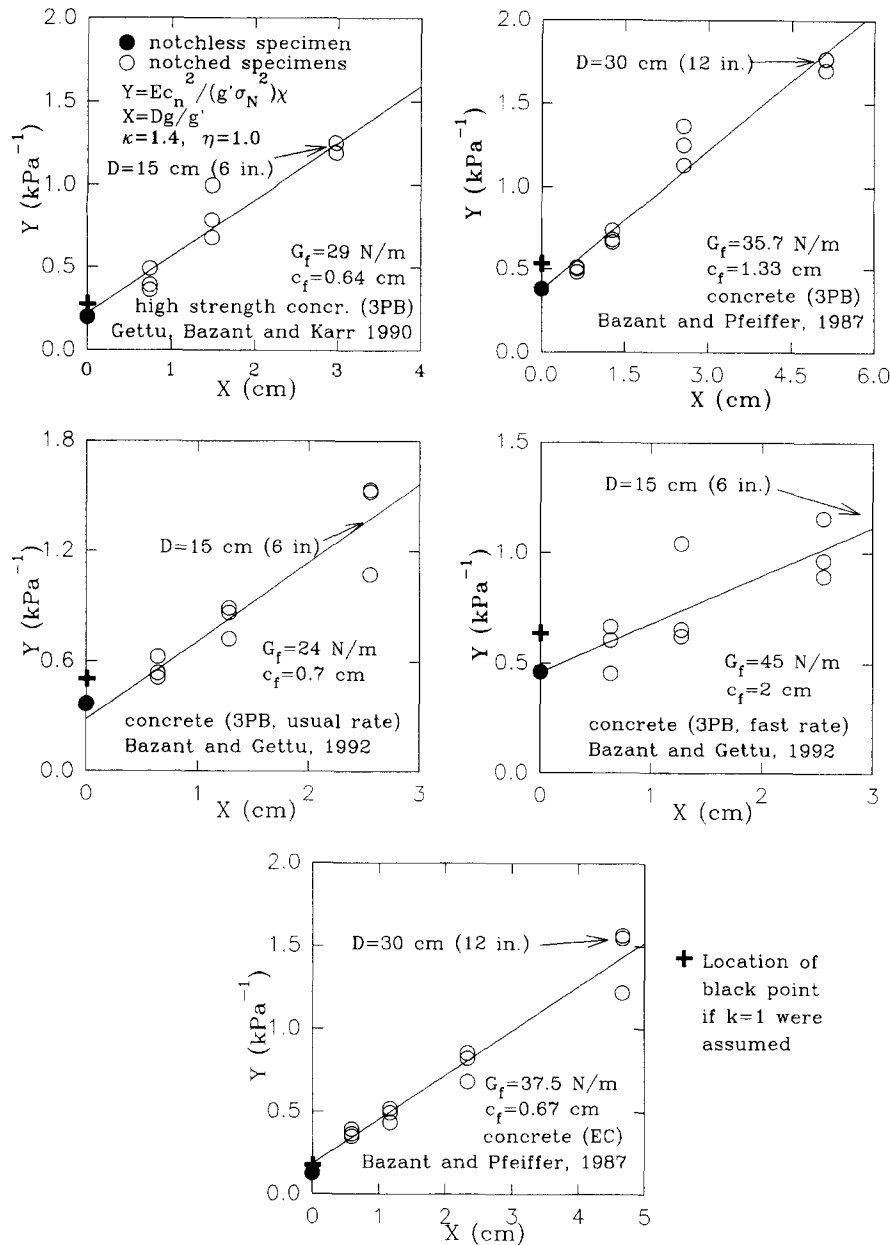


FIGURE 4. Size effect linear regression plots of typical published test data (empty points), their regression lines, and predictions by Type III method for notchless specimens.

fect, with the fractality effect implied only in the values of Weibull parameters (which cannot be predicted theoretically but must be calibrated by experiment). The reason is that if microcracks controlled failure, the failure would have to occur right at the start of macroscopic fracture growth, without any stable crack growth. Because the concrete structures of interest exhibit large stable crack growth, such a failure mode is an unrealistic hypothesis.

Diffusion Size Effects

Diffusion phenomena such as water transport (drying) and heat transport caused by hydration and by envi-

ronmental fluctuations engender time-dependent size effects, which must be avoided in fracture testing. To eliminate these size effects, all the specimens should have the same thickness. The drying size effect is also eliminated if the specimens are sealed during their curing and the test is made right after stripping the seals.

Wall Effect

The wall effect is due to the fact that (1) the surface layer of concrete has a different aggregate content and size distribution than the interior, (2) the fluctuating microstresses normal to the surface are nonzero in the interior but zero on the surface, and (3) out-of-plane

shear lips can develop at the surface ending of crack front edge. This has no appreciable influence on the observed size effect if the thickness of all specimens is the same.

Acknowledgment

Partial financial support from the National Science Foundation under Grant MSS-911447-6 to Northwestern University and from the ACBM Center at Northwestern University is gratefully acknowledged.

References

1. ACI Committee 446. In *Fracture Mechanics of Concrete Structure*; Bažant, Z.P., Ed. Elsevier Applied Science: New York, 1992; pp 4-144.
2. Nakayama, J. *J. Am. Ceramic Soc.* **1965**, 48(11), 583-587.
3. Tattersall, H.G.; Tappin, G. *J. Mater. Sci.* **1966**, 1(3), 296-301.
4. Hillerborg, A. *Materials and Structures* **1985**, 18(106), 291-296.
5. Hillerborg, A. *Materials and Structures* **1985**, 18(107), 407-413.
6. Planas, J.; Elices, M.; Guinea, G.V. *Int. J. Fracture* **1993**, 63(2), 173-187.
7. RILEM Recommendation. *Materials and Structures* **1990**, 23, 461-465.
8. Bažant, Z.P. In *SEM-RILEM International Conference on Fracture of Concrete and Rock*, Houston, Texas, June 1987; Shah, S.P.; Swartz, S.E., Eds.; Society for Experimental Mechanics, 1987; pp 390-402.
9. Bažant, Z.P.; Pfeiffer, P.A. *ACI Mater. J.* **1987**, 84(6), 463-480.
10. Bažant, Z.P.; Kazemi, M.T. *Int. J. Fracture* **1990**, 44, 111-131.
11. Bažant, Z.P. In *IUTAM Prager Symposium on Mechanics of Geomaterials: Rocks, Concretes, Soils*; Bažant, Z.P., Ed.; Northwestern University: Evanston, Illinois, 1983; pp 281-316.
12. Bažant, Z.P. *ASCE J. Eng. Mechanics* **1984**, 110, 518-535.
13. Bažant, Z.P.; Cedolin, L. *Stability of Structures: Elastic, Inelastic, Fracture and Damage Theories*; Oxford University Press: New York, 1991.
14. Jenq, Y.S.; Shah, S.P. *ASCE J. Eng. Mechanics* **1985**, 111(4), 1227-1241.
15. Wells, A.A. In *Symposium on Crack Propagation*; Cranfield, vol. 1; 1961; pp 210-230.
16. Cottrell, A.H. *Iron and Steel Institute Special Report*, 69; 1963, p 281.
17. Ouyang, C.; Shah, S.P. *J. Am. Ceramic Soc.* **1991**, 74, 2831-2836.
18. Planas, J.; Elices, M. In *Cracking and Damage*; Mazars, J.; Bažant, Z.P., Eds. Elsevier: London, 1989; pp 462-476.
19. Planas, J.; Guinea, G.V.; Elices, M. *Report to ACI-SEM Joint Task Group on Fracture Testing of Concrete*, Universidad Politecnica de Madrid (June); 1994; p 6.
20. Guinea, G.V.; Planas, J.; Elices, M. *Materials and Structures* **1994**, 27, 99-105.
21. Planas, J.; Elices, M.; Toribio, J. In *Fracture of Concrete and Rock: Recent Developments*; Shah, S.P.; Swartz, S.; Barr, B.I.G., Eds.; Elsevier Applied Science: London, 1989; pp 203-212.
22. Tang, T. Private communication to Z.P. Bažant, Texas Transportation Institute, Texas A&M University, 1994.
23. RILEM Recommendation. *Materials and Structures* **1985**, 18(106), 00-00.
24. Li, Z. Private communication to Z.P. Bažant, Northwestern University, Evanston, Illinois, 1995.
25. Bažant, Z.P.; Li, Z. *J. Struct. Eng.* **1995**, 121(4), 739-746.
26. Bažant, Z.P.; Li, Z. *J. Eng. Mechanics* **1995**, 121, in press.
27. Bažant, Z.P. *J. Struct. Eng.* **1994**, 120(8), 2555-2558.
28. Bažant, Z.P.; Gettu, R.; Kazemi, M.T. *Int. J. Rock Mechanics and Mining Sci.* **1991**, 28(1), 43-51.
29. Karihaloo, B. *Fracture Mechanics and Structural Concrete*; Longman: London, 1995.
30. Karihaloo, B.L.; Nallathambi, P. In *Fracture Mechanics Test Methods for Concrete*, Shah, S.P.; Carpinteri, A., Eds.; Chapman and Hall: London, 1991; pp 1-86.
31. Bažant, Z.P. In *Dei Poli Anniversary Volume*; Cedolin, L.; et al., Eds.; Politecnico di Milano: Italy, 1995; pp 335-338.
32. Bažant, Z.P. In *U.S.-Japan Seminar on Finite Element Analysis of Reinforced Concrete Structures*, vol. 1; Tokyo, 1985; pp 47-69.
33. Bažant, Z.P. In *Fracture Mechanics of Concrete Structures*; Wittmann, F.H., Ed.; Aedificatio Publishers: Freiburg, Germany, 1995; pp 515-534.
34. Bažant, Z.P. *ASCE J. Mater. Tech.* **1995**, 117, 361-367.
35. Bažant, Z.P.; Xi, Y.; Reid, S.G. *ASCE J. Eng. Mechanics* **1991**, 117(11), 2609-2622.
36. Carpinteri, A.; Chiaia, B.; Ferro, G. In *Size Effect in Concrete Structures*; Mihashi, M.; Okamura, H.; Bažant, Z.P., Eds.; E & FN Spon: London-New York, 1994; pp 193-206.
37. Carpinteri, A.; Chiaia, B. In *Fracture Mechanics of Concrete Structures*; Wittmann, F.H., Ed.; Aedificatio Publishers: Freiburg, Germany, 1995; pp 581-596.